



# In vivo assessment of OXPHOS capacity using 3 T CrCEST MRI in Friedreich's ataxia

Gayatri Maria Schur<sup>1,2</sup> · Julia Dunn<sup>1</sup> · Sara Nguyen<sup>1</sup> · Anna Dedio<sup>1</sup> · Kristin Wade<sup>1</sup> · Jaclyn Tamaroff<sup>1</sup> · Nithya Mitta<sup>1</sup> · Neil Wilson<sup>3</sup> · Ravinder Reddy<sup>3</sup> · David R. Lynch<sup>4</sup> · Shana E. McCormack<sup>1,5,6</sup>

Received: 2 August 2021 / Accepted: 24 September 2021 / Published online: 15 October 2021  
© The Author(s) 2021

## Abstract

**Background** Friedreich's ataxia (FRDA) is a neurodegenerative disease caused by decreased expression of frataxin, a protein involved in many cellular metabolic processes, including mitochondrial oxidative phosphorylation (OXPHOS). Our objective was to assess skeletal muscle oxidative metabolism in vivo in adults with FRDA as compared to adults without FRDA using chemical exchange saturation transfer (CrCEST) MRI, which measures free creatine (Cr) over time following an in-magnet plantar flexion exercise.

**Methods** Participants included adults with FRDA ( $n = 11$ ) and healthy adults ( $n = 25$ ). All underwent 3-Tesla CrCEST MRI of the calf before and after in-scanner plantar flexion exercise. Participants also underwent whole-body dual-energy X-ray absorptiometry (DXA) scans to measure body composition and completed questionnaires to assess physical activity.

**Results** We found prolonged post-exercise exponential decline in CrCEST ( $\tau$ Cr) in the lateral gastrocnemius (LG, 274 s vs. 138 s,  $p = 0.01$ ) in adults with FRDA (vs. healthy adults), likely reflecting decreased OXPHOS capacity. Adults with FRDA (vs. healthy adults) also engaged different muscle groups during exercise, as indicated by muscle group-specific changes in creatine with exercise ( $\Delta$ CrCEST), possibly reflecting decreased coordination. Across all participants, increased adiposity and decreased usual physical activity were associated with smaller  $\Delta$ CrCEST.

**Conclusion** In FRDA, CrCEST MRI may be a useful biomarker of muscle-group-specific decline in OXPHOS capacity that can be leveraged to track within-participant changes over time. Appropriate participant selection and further optimization of the exercise stimulus will enhance the utility of this technique.

**Keywords** Friedreich's ataxia · Magnetic resonance imaging · Skeletal muscle · OXPHOS · Oxidative metabolism · Exercise · Mitochondrial disorders

✉ Gayatri Maria Schur  
gayatri.schur@nyulangone.org

<sup>1</sup> Division of Endocrinology and Diabetes, The Children's Hospital of Philadelphia, Philadelphia, PA 19104, USA

<sup>2</sup> Medical Scientist Training Program, New York University Grossman School of Medicine, Vilcek Institute of Graduate Biomedical Sciences, 550 First Avenue, MSB 228, New York, NY 10016, USA

<sup>3</sup> Center for Magnetic Resonance and Optical Imaging, Department of Radiology, University of Pennsylvania, Philadelphia, PA 19104, USA

<sup>4</sup> Division of Neurology, The Children's Hospital of Philadelphia, Philadelphia, PA 19104, USA

<sup>5</sup> Department of Pediatrics, Perelman School of Medicine, University of Pennsylvania, Philadelphia, PA 19104, USA

<sup>6</sup> Department of Neurology, Perelman School of Medicine, University of Pennsylvania, Philadelphia, PA 19104, USA

## Abbreviations

3 T	3 Tesla
BMI	Body mass index
Cr	Creatine
CrCEST	Creatine chemical exchange saturation transfer
$\Delta$ CrCEST	Change in CrCEST with exercise
DXA	Dual-energy X-ray absorptiometry
FRDA	Friedreich's ataxia
LG	Lateral gastrocnemius
MG	Medial gastrocnemius
MRI	Magnetic resonance imaging
MRS	Magnetic resonance spectroscopy
MTR <sub>asym</sub>	Magnetization transfer asymmetry
OXPHOS	Oxidative phosphorylation
PCr	Phosphocreatine

Sol Soleus  
 $\tau_{Cr}$  Post-exercise CrCEST recovery exponential time constant

expected to impact muscle metabolism, including body composition and physical activity.

## Introduction

Friedreich's ataxia (FRDA) is a rare neurodegenerative disease caused by GAA triplet-repeat expansions in the *FXN* gene, which encodes the protein frataxin [1]. Frataxin regulates the assembly of iron–sulfur clusters necessary for mitochondrial oxidative phosphorylation (OXPHOS) [2]. The GAA triplet-repeat expansion leads to decreased *FXN* expression and therefore decreased frataxin levels and impaired mitochondrial OXPHOS capacity. Individuals with FRDA have impaired skeletal muscle OXPHOS capacity as measured by  $^{31}\text{P}$  magnetic resonance spectroscopy (MRS), which has historically been used to assess OXPHOS capacity in vivo by measuring changes in phosphocreatine (PCr) over time in response to exercise [3, 4]. However, the limited spatial resolution of  $^{31}\text{P}$ -MRS makes assessment of muscle-group-specific OXPHOS capacity challenging. This is a significant disadvantage of  $^{31}\text{P}$ -MRS because different muscle groups may differ in myofiber type composition, and different myofiber types have distinct metabolic properties and mitochondrial OXPHOS capacity [5].

Chemical exchange saturation transfer (CEST) MRI is a contrast enhancement technique that can indirectly measure endogenous metabolites through their exchange with bulk water [6, 7]. When saturation pulses are applied to the amine protons of creatine, this saturated magnetization exchanges with bulk water protons in the surrounding tissue, resulting in a decrease in water signal proportional to Cr concentration. Using this creatine-weighted CEST contrast (CrCEST), free creatine (Cr) can be measured over time in response to a provocative exercise stimulus to indirectly assess skeletal muscle oxidative metabolism [8]. As compared to  $^{31}\text{P}$ -MRS, CrCEST MRI has the added benefit of enhanced sensitivity that allows for high spatial resolution imaging, making muscle group-specific assessment of metabolism possible. In addition, CrCEST can be performed with a standard  $^1\text{H}$  coil, while  $^{31}\text{P}$ -MRS requires multinuclear hardware not as widely available [6].

Recently, our group detected differences in OXPHOS capacity in the medial gastrocnemius muscle between adults with diverse primary mitochondrial disorders (mostly non-FA) and healthy adults using CrCEST at 7 T [9]. In this study, we used the CrCEST technique to assess skeletal muscle OXPHOS capacity in individuals with FRDA relative to individuals without FRDA at 3 T, a more widely available field strength. We aimed to characterize the relationship between OXPHOS capacity and candidate clinical factors

## Materials and methods

*Study design and participants.* This study was conducted under an approved Institutional Review Board protocol. Written informed consent for each participant was obtained. Adults (ages 18–65 years) with a confirmed genetic diagnosis of FRDA, without diabetes mellitus, were recruited for a cross-sectional, observational metabolic phenotyping study (NCT02920671) that included CrCEST imaging. Healthy adults without diabetes mellitus were recruited to generate a control cohort with a similar distribution of age, sex, body mass index (BMI), and population ancestry as individuals with FRDA.

*Waist circumference and body composition.* Waist circumference was measured at the upper aspect of the iliac crest. Body composition (whole body and regional) was assessed using the Horizon A Platform (Hologic, Inc., Bedford MA) with Apex software v5.5 at the Children's Hospital of Philadelphia Growth and Nutrition Laboratory. Outcomes assessed included whole-body lean and fat mass, and leg lean and fat mass.

*Physical activity.* Adults completed the Chronic Renal Insufficiency Cohort (CRIC) Physical Activity Questionnaire to generate estimates of usual physical activity, including time spent in light-, moderate-, and heavy-intensity exercise, intentional exercise, and total physical activity [10].

*Magnetic resonance imaging.* CrCEST imaging was performed using a 15-channel  $^1\text{H}$  Tx/Rx knee coil (Quality Electrodynamics, Mayfield Village, OH, USA) on a 3 T whole-body scanner (MAGNETOM Prisma, Siemens Healthcare, Erlangen, Germany) at the University of Pennsylvania (Philadelphia, PA). CrCEST imaging parameters were as follows: TR/TE = 4.7/2.3 ms, slice thickness = 10 mm, flip angle =  $10^\circ$ , saturation  $B_{1_{\text{rms}}}$  = 3  $\mu\text{T}$ , saturation duration = 500 ms, in plane resolution =  $1.25 \times 1.25 \text{ mm}^2$ , matrix size =  $128 \times 128$ , field of view =  $160 \times 160 \text{ mm}^2$ . Time between saturation was 4 s, and offsets were acquired at /pm 1.5, 1.8, and 2.1 ppm relative to water. Water saturation shift reference (WASSR) and  $B_1^+$  maps were acquired, to correct for  $B_0$  and  $B_1$  field inhomogeneities [11, 12].

The same exercise-based imaging procedures were as follows. First, five baseline images of the right calf were acquired with a temporal resolution of 24 s. Then, participants performed a plantar flexion exercise for 2 min inside the scanner using an MR-compatible ergometer (Penn), held at a fixed resistance. The individualized exercise stimulus was designed to be mild; prior to scanning, capacity to perform the exercise was assessed. In healthy adult volunteers, 12 psi was used. In individuals with FRDA with limited

exercise capacity, resistance was decreased to either 8 or 4 psi, as appropriate, if participants could not easily depress the pedal with the 12-psi resistance. All participants were coached to complete the exercise at a frequency of 45 repetitions per minute, with adherence verified visually. Participants with limited capacity to perform the exercise were directed to keep cadence to the extent possible. The goal of the exercise stimulus was to deplete PCr and increase Cr sufficiently to measure post-exercise Cr decline. Eight minutes of post-exercise images were acquired at the same temporal resolution of 24 s.

**Image processing.** Image processing was performed using an in-house written MATLAB (version 2019a) program [13]. CEST contrast ( $MTR_{\text{asym}}$ ) is computed via z-spectra asymmetry analysis [6]. To determine  $MTR_{\text{asym}}$  for individual muscle groups, anatomical images were manually segmented for the muscles most involved in the plantar flexion movement, which included the lateral gastrocnemius (LG), medial gastrocnemius (MG), and soleus (Sol) muscles in the calf, and these segmentations were applied to the CrCEST maps.  $MTR_{\text{asym}}$  of the voxels included in each segmented muscle group were then averaged for each timepoint. For a given muscle, resting CrCEST (prior to exercise) was computed as the average CrCEST from the baseline images, representing the free creatine concentration at rest. Change in CrCEST with exercise ( $\Delta\text{CrCEST}$ ) was computed as the change between resting CrCEST and the value of  $MTR_{\text{asym}}$  at the first post-exercise timepoint, representing the change in free creatine with exercise. According to the kinetics of the phosphocreatine (PCr) shuttle, decline in free creatine concentration after exercise is typically modelled as an exponential function [8]. Thus, the post-exercise exponential decline in CrCEST ( $\tau\text{Cr}$ ) is the main outcome reflecting OXPHOS capacity. CrCEST imaging has sufficiently high anatomic resolution to perform muscle-group-specific analyses; thus,  $\tau\text{Cr}$  was computed by fitting muscle-specific  $MTR_{\text{asym}}$  timeseries to an exponential model.

Based on our previous experience, physiologically relevant values of  $\tau\text{Cr}$  are expected to fall between ~50 and 300 s [9].  $\tau\text{Cr}$  estimates less than one inter-scan interval (24 s) were excluded because of the limited temporal resolution. Values of  $\tau\text{Cr}$  greater than 1,000 s, well above the upper range of the  $\tau\text{Cr}$  distribution (over all measurements, the 95th percentile in healthy controls was 399 s and in individuals with FA was 449 s) and beyond the post-exercise scan duration (480 s), were also excluded as implausible and likely due to an insufficient exercise response.

**Statistical analyses.** The Shapiro–Wilk test was used to test the normality of distribution for CrCEST imaging outcomes. Kruskal–Wallis tests were performed in non-normally distributed outcome measures. Linear mixed-effects models were used to assess the effect of disease status on each muscle-group-specific CrCEST imaging outcome,

adjusting statistically for clinical covariates, while also accounting for subject-specific random effects. For the outcomes assessed, if an interaction effect between disease status and muscle group was detected, suggesting that the impact of disease status on the CrCEST outcome varied between muscle groups, then linear regression models were built for each muscle group (LG, MG, Sol) separately to investigate the effect of covariates. In all models, subject is included as a random effect and sex, age, and disease status were included as fixed effects. Sex and age were included because skeletal muscle composition varies with these clinical characteristics.

Statistical models testing the outcome of resting CrCEST included age, sex, disease status, muscle group, and the following additional fixed effects: no additional effects (Model 1); BMI (Model 2); height, and right leg lean tissue mass (Model 3); height and right leg fat mass (Model 4). Statistical models testing the outcome of  $\Delta\text{CrCEST}$  included age, sex, disease status, and the following additional covariates: no additional covariates (Model 1); total physical activity (Model 2); waist circumference (Model 3). Statistical models testing the outcome of  $\tau\text{Cr}$  included sex, age, disease status and the following additional covariates: no additional covariates (Model 1);  $\Delta\text{CrCEST}$  and resting CrCEST (Model 2); total physical activity (Model 3). Statistical interactions between disease status and muscle group were detected in mixed-effects models of both  $\Delta\text{CrCEST}$  and  $\tau\text{Cr}$ , so linear regression models of each outcome were built for each muscle group separately. All statistical analyses were done in RStudio (Version 1.1.383), and statistical significance was taken to be a two-sided  $p$  value of  $<0.05$ .

## Results

**Participants.** Characteristics of study participants are summarized in Table 1. By design, there were similar proportions of individuals who were obese between FRDA and control cohorts, and a nominally higher proportion of individuals with FRDA were in the overweight relative to normal weight category as compared to controls. Fifty-five percent of individuals with FRDA and 40% of controls had increased waist circumference for age, defined as  $>88$  cm for females and  $>102$  cm for males [14]. Individuals with FRDA reported spending less time in total weekly physical activity, as well as less time in light- and heavy-intensity exercise as compared to control participants.

## CrCEST imaging

CrCEST imaging outcomes (resting CrCEST,  $\Delta\text{CrCEST}$  following exercise, and  $\tau\text{Cr}$ ) are summarized in Table 2. Individual CrCEST maps and corresponding time series are

**Table 1** Characteristics of adult subjects (healthy volunteers and FRDA)

Characteristic	Healthy volunteers ( <i>n</i> = 25)	Friedreich's ataxia ( <i>n</i> = 11)
Sex (%female, <i>n</i> )	44% (11)	36% (4)
Age (years)	29 (25–39)	27 (23–39)
GAA repeats (bp)	NA	633 (467–741)
<i>Anthropometrics and body composition</i>		
BMI (kg/m <sup>2</sup> )	24.4 (22.0–26.6)	26.9 (24.1–29.4)
BMI Category (kg/m <sup>2</sup> )		
Underweight, < 18.5 (% , <i>n</i> )	0% (0)	9% (1)
Normal weight, 18.5–24.9 (% , <i>n</i> )	56% (14)	18% (2)
Overweight, 25–30 (% , <i>n</i> )	24% (8)	55% (6)
Obese, > 30 (% , <i>n</i> )	12% (3)	18% (2)
Fat Mass Index (kg/m <sup>2</sup> )	2.7 (2.3–3.7)	3.8 (2.4–5.2)
Waist circumference (cm)	93 (88–100)	99 (89–110)
Proportion with increased (high-risk) sex-specific weight circumference (%increased, <i>n</i> )	40% (10)	55% (6)
<i>Physical activity and exercise</i>		
Total physical activity (MET-hrs/wk)	<b>19.2 (16.1–26.7)</b>	<b>11.1 (4.0–13.0)</b>
Intentional exercise (MET-hrs/wk)	5.9 (2.2–12.2)	2.8 (0.0–5.3)
Light-intensity exercise (MET-hrs/wk)	<b>11.1 (7.0–14.9)</b>	<b>3.5 (0.8–6.9)</b>
Moderate-intensity exercise (MET-hrs/wk)	3.6 (2.1–7.7)	1.3 (0.0–6.0)
Heavy-intensity exercise (MET-hrs/wk)	<b>1.3 (0.0–6.9)</b>	<b>0.0 (0.0–0.0)</b>

Means ± standard deviations are shown for normally distributed variables, and medians ± interquartile intervals are shown non-normally distributed variables. Normality of distribution was assessed using a Shapiro–Wilk test. Values in bold text indicate a statistically significant difference ( $p < 0.05$ ) between individuals with FRDA versus healthy volunteers by Student's *t* test or Kruskal–Wallis test, as appropriate. The number of GAA repeats in the FXN gene on the least affected allele correlates with earlier age of onset, more rapid disease progression, and severity of symptoms, but does not account for all phenotypic variability [1]

**Table 2** Adult CrCEST MRI results, univariate analyses

	Healthy controls ( <i>n</i> = 22)	Friedreich's ataxia ( <i>n</i> = 10)
Resting CrCEST (%asymmetry, index of free Cr concentration)		
LG	6.2 (5.3–8.2)	5.9 (4.9–6.4)
MG	5.9 (5.4–7.5)	6.3 (5.7–7.0)
Sol	6.6 (6.0–7.0)	7.0 (6.1–7.4)
ΔCrCEST with exercise (%asymmetry)		
LG	8.9 (6.0–10.4)	5.2 (2.9–9.1)
MG	5.0 (4.5–5.8)	3.5 (1.2–5.5)
Sol	3.4 (2.8–4.7)	3.9 (1.7–6.6)
τCr (seconds, index of OXPHOS capacity)		
LG	<b>138 (85–226)</b>	<b>274 (221–309)</b>
MG	184 (90–263)	269 (240–342)
Sol	254 (184–309)	210 (149–266)

Medians ± interquartile intervals are shown for non-normally distributed variables. Normality of distribution was assessed using a Shapiro–Wilk test. Values in bold text indicate a statistically significant difference ( $p < 0.05$ ) between individuals with FRDA versus healthy volunteers by Kruskal–Wallis test. Total participant numbers reflect that 3 participant scans (1 case and 2 controls) were excluded due to technical limitations, including motion artifacts, shimming and other image acquisition errors. τCr values less than one scan time (24 s) were excluded, including two observations in the MG

LG: lateral gastrocnemius, MG: medial gastrocnemius, Sol: soleus

shown for two representative participants in Fig. 1, including a healthy 25yo male and a 30yo male with FRDA. Three scans (1 case and 2 controls) were excluded due to data collection limitations, including significant motion artifacts and field inhomogeneity correction errors. Two observations of  $\tau_{Cr}$  in the MG were less than one scan time (24 s) and were, therefore, excluded. Otherwise, other fitted values fell within the specified plausible range of 24–1,000 s and were therefore included in the analysis.

**Resting CrCEST.** In univariate analyses, we did not detect a difference between FRDA and controls in resting CrCEST, an index of free creatine concentration at rest (Table 2, Supplementary Fig. 1). We also did not detect the presence of

any muscle group-specific interaction effects with disease status, so we investigated the effects of other potentially relevant covariates on resting CrCEST analyzing all muscle groups together. Independent of disease status, resting CrCEST was higher in the soleus as compared to the LG in all models ( $p=0.002$ ) (Table 3). Also independent of disease status, higher BMI ( $\beta = -0.11$ ,  $p=0.006$ ) was associated with lower resting CrCEST (Table 3, Model 2). To better understand the relationship between BMI and resting CrCEST, we examined models including more detailed body composition measures from DXA scans. Both lean mass ( $\beta = -0.42$ ,  $p=0.025$ ) and fat mass ( $\beta = -0.32$ ,  $p=0.007$ ) in the right leg were also associated with lower resting

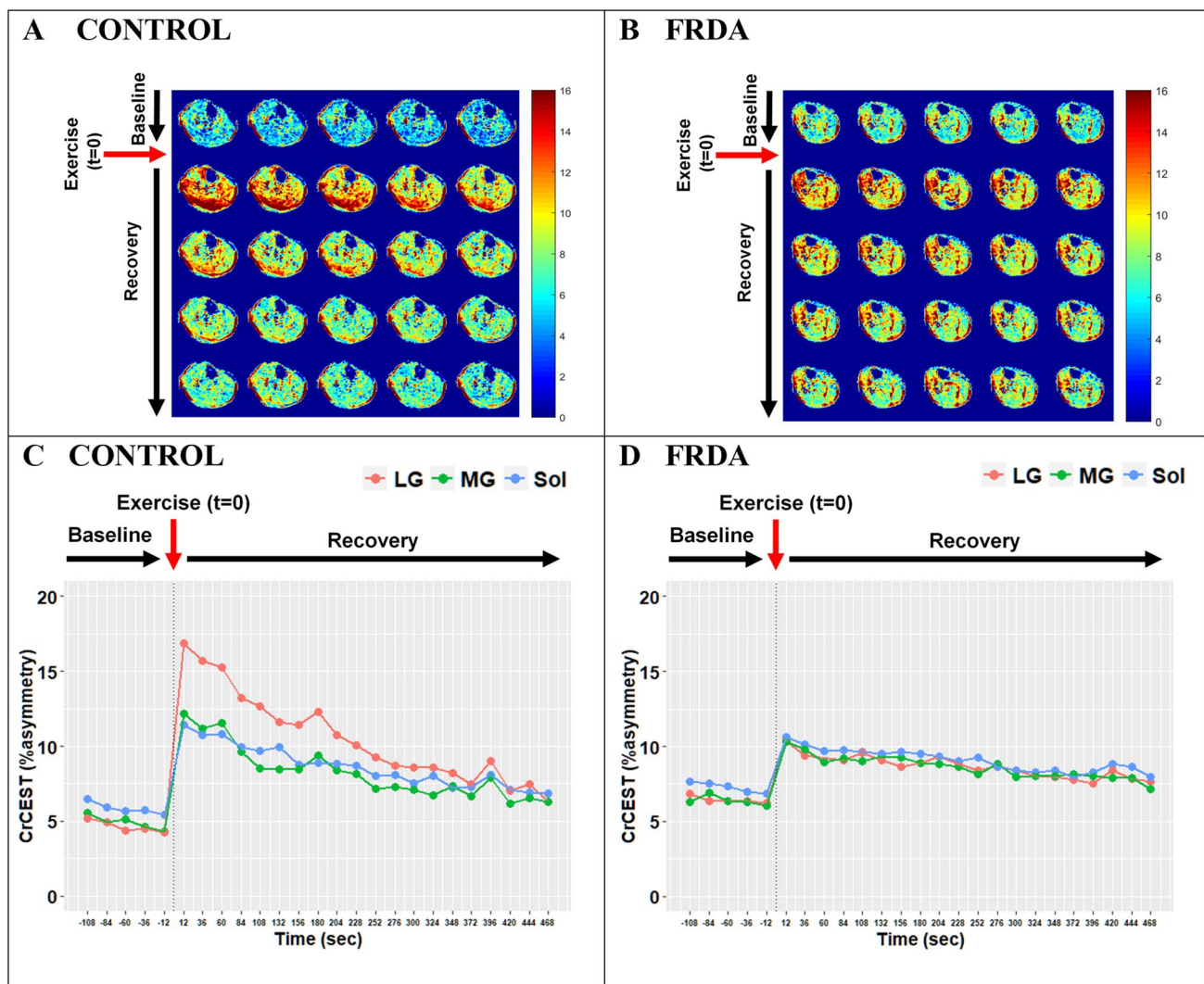


**Fig. 1** CrCEST over time for a healthy 25yo male and a 30yo male with FRDA, respectively. (A, B) Maps of CrCEST (%asymmetry), rest-exercise-recovery protocol for (A) healthy 25yo male where  $\tau_{Cr}$ =269 s, 263 s, 287 s and (B) 30yo male with FRDA where  $\tau_{Cr}$ =741 s, 451 s, 367 s for the LG, MG, and soleus, respectively. The color bar indicates the intensity of the CrCEST signal, in pro-

portion to the concentration of Cr in the muscle. (C, D) CrCEST over time for the same participants; prolonged recovery corresponds to decreased OXPHOS capacity. CrCEST in the LG at  $t=60$  s was omitted from the time series plot in Fig. 1D due to an error in image acquisition at that timepoint but was included in model fitting. LG: lateral gastrocnemius, MG: medial gastrocnemius, Sol: soleus

**Table 3** Adults with FRDA vs. healthy controls, mixed-effects regression model of resting CrCEST (%asymmetry, an index of free creatine concentration)

	Model 1 $\beta$ , [CI]	Model 2 $\beta$ , [CI]
Age (years)	0.005 [−0.03, 0.03]	−0.01 [−0.04, 0.02]
Male sex (vs. female)	−0.85 [−1.8, 0.07]	<b>−1.1*</b> [−1.9, −0.27]
FRDA (vs. no FRDA)	−0.27 [−1.1, 0.62]	0.13 [−0.67, 0.93]
BMI (kg/m <sup>2</sup> )	–	<b>−0.11**</b> [−0.19, −0.043]
Muscle Group		
LG (reference)	–	–
MG	0.07 [−0.23, 0.38]	0.07 [−0.23, 0.38]
Soleus	<b>0.50**</b> [0.19, 0.81]	<b>0.50**</b> [0.19, 0.81]

In each model, subject is included as a random effect and clinical covariates as fixed effects. The following fixed effects were included: Model 1, age, sex, disease status, muscle group; Model 2, age, sex, disease status, BMI, and muscle group. For both models,  $n=32$  participants contributed a total of  $n=96$  observations. No observations were excluded.  $\beta$  coefficient values are shown, with corresponding 95% confidence intervals. Results in bold text indicate statistically significant  $\beta$  coefficient values: \* $p < 0.05$ ; \*\* $p < 0.01$ ; \*\*\* $p < 0.001$

LG: lateral gastrocnemius, MG: medial gastrocnemius, Sol: soleus

CrCEST in adults when accounting statistically for age, sex, and height. Because larger individuals tend to have more fat mass as well as more lean mass, we tested a model including both lean and fat mass in the leg, but likely due to the sample size, we were unable to discern which of these contributed most to resting CrCEST. Of note, resting CrCEST remained

higher in the soleus compared to the LG when accounting for leg lean and fat mass. With respect to other covariates, in our previous study of adults with mitochondrial disease, we detected a positive association between intentional exercise and resting CrCEST in the soleus, but we did not detect an association between physical activity and resting CrCEST in FRDA in this study.<sup>9</sup>

$\Delta$ CrCEST. In univariate analyses, we did not detect differences between FRDA and controls in  $\Delta$ CrCEST, a measure reflecting change in free creatine with exercise, in any muscle group (Table 2, Supplementary Fig. 2). This is by design, since our priority outcome measure is post-exercise exponential decline in CrCEST or  $\tau$ Cr, which reflects OXPHOS capacity, and we sought to individualize exercise resistance to produce provocative changes in CrCEST with exercise of approximately similar magnitude between cases and controls. However, mixed-effects regression analyses showed a significant interaction effect between disease status and muscle group on exercise  $\Delta$ CrCEST in adults ( $p < 0.001$  for difference between LG and Sol), indicating that individuals with FRDA had different patterns of muscle use with exercise as compared to controls. Specifically,  $\Delta$ CrCEST with exercise was nominally smaller in the LG and MG in FRDA versus in controls, but  $\Delta$ CrCEST with exercise in soleus was similar. (Supplementary Fig. 2). This can also be visually observed in individual CrCEST maps, including in Fig. 1, where the control predominantly engages the LG, while the participant with FRDA has a more uniform response across the posterior lower leg.

We next assessed the effects of several clinical covariates on  $\Delta$ CrCEST within each muscle group using linear regression models (Table 4, Supplementary Table 1). In our linear models, self-reported time spent in total weekly

**Table 4** Adults with FRDA vs. healthy controls, linear regression model of  $\Delta$ CrCEST with exercise (%asymmetry, an index of free creatine concentration) in the lateral gastrocnemius, where a larger  $\Delta$ CrCEST represents a larger change with exercise

Covariate	Model 1 $\beta$ [CI]	Model 2 $\beta$ [CI]	Model 3 $\beta$ [CI]
Age (years)	0.03 [−0.09, 0.16]	−0.04 [−0.16, 0.09]	0.02 [−0.09, 0.14]
Male sex (vs. female)	1.6 [−1.8, 5.0]	0.7 [−2.5, 3.0]	1.1 [−2.2, 4.4]
FRDA (vs. no FRDA)	−2.8 [−6.1, 0.4]	−0.47 [−4.1, 3.1]	−1.8 [−5.1, 1.5]
Total Physical Activity (MET-hrs/wk)	–	<b>0.20*</b> [0.03, 0.37]	–
Waist Circumference (cm)	–	–	−0.09 [−0.19, 0.01]

For all models,  $n=32$  participants contributed a total of  $n=32$  observations. No observations were excluded. The following covariates were included: Model 1, age, sex, and disease status (no additional covariates); Model 2, age, sex, disease status, and total physical activity; Model 3, age, sex, disease status, and waist circumference.  $\beta$  coefficient values are shown, with corresponding confidence intervals. Results in bold text indicate statistically significant  $\beta$  coefficient values: \* $p < 0.05$ ; \*\* $p < 0.01$ ; \*\*\* $p < 0.001$

physical activity (MET-hours/week) was associated with a greater  $\Delta\text{CrCEST}$  in the LG ( $\beta = 0.18$ ,  $p = 0.02$ ), independent of disease status, sex and age (Table 4). We also found that higher waist circumference (cm) was associated with smaller  $\Delta\text{CrCEST}$  in the MG ( $\beta = -0.06$ ,  $p = 0.005$ ) and soleus muscles ( $\beta = -0.06$ ,  $p = 0.008$ ) across both cases and controls (Supplementary Table 1); a similar pattern was observed in LG, but this result did not reach statistical significance.

**Post-exercise  $\tau\text{Cr}$ .** In univariate analyses, individuals with FRDA had a prolonged  $\tau\text{Cr}$  in the LG relative to individuals without FRDA (274 s vs. 138 s,  $p = 0.01$ ), suggestive of decreased OXPHOS capacity in this muscle group (Table 2). In the MG,  $\tau\text{Cr}$  was 262 s vs. 171 s (nominally longer, but not statistically different), and in soleus 210 s vs. 254 s (similar), in individuals with FRDA and controls, respectively. CrCEST time series for all three muscle groups, averaged for FRDA vs. control, are illustrated in Fig. 2. Dot plots for post-exercise  $\tau\text{Cr}$  across all three muscle groups are shown in Fig. 3.

In mixed-effects regression analyses of  $\tau\text{Cr}$ , an interaction effect between disease status and muscle group was detected ( $p < 0.001$  for the difference between LG and Sol). The presence of this interaction indicates that the impact of disease status on  $\tau\text{Cr}$  varies by muscle group, and here, means that the disease-specific differences in post-exercise  $\tau\text{Cr}$  in LG were not detected in the Sol. We next investigated the effects of potentially relevant clinical covariates including age, sex, BMI, and self-reported physical activity, and technical covariates including resting CrCEST and  $\Delta\text{CrCEST}$ , in successive regression models to test whether the effect of FRDA on post-exercise  $\tau\text{Cr}$  we observed may be explained by FRDA-related differences in these covariates (Table 5, Supplementary Table 2).

Linear regression models showed a significant effect of FRDA on  $\tau\text{Cr}$  in the LG in all models including the technical covariates resting CrCEST and  $\Delta\text{CrCEST}$ , thus these covariates did not explain the effect of disease on  $\tau\text{Cr}$  (Table 5). Model-derived estimates indicate that  $\tau\text{Cr}$  is prolonged in the LG by 131 s ( $p = 0.01$ , 95% CI = 28–234 s) in FRDA relative to unaffected individuals, when accounting statistically for sex and age. As a point of reference, median  $\tau\text{Cr}$  in the LG was 138 s (IQR = 85–227 s) in controls and 274 s (IQR = 221–309 s) in FRDA. Previously, in our study of adults with mitochondrial disease, we detected a correlation between self-reported time spent weekly in intentional exercise and post-exercise  $\tau\text{Cr}$  [9]. In this study, we detected an association between self-reported physical activity and post-exercise  $\tau\text{Cr}$  in the MG only, independent of disease status (Supplementary Table 2). Further, the effect of disease status on  $\tau\text{Cr}$  in the LG became less apparent when accounting for total

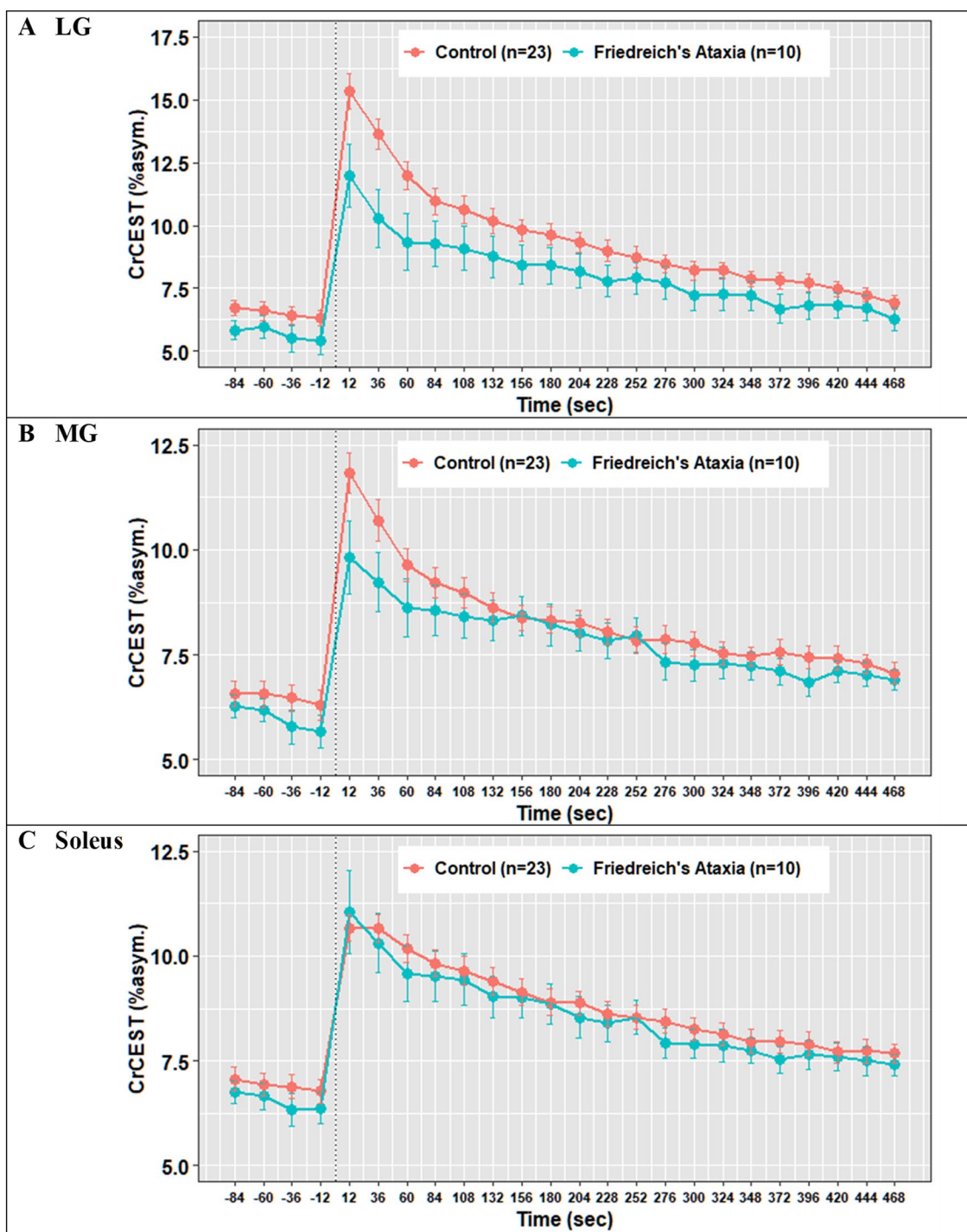
physical activity, suggesting that physical activity differences may partially explain the effect of FRDA on  $\tau\text{Cr}$ .

## Discussion

The main goal of this study was to test a novel metabolic imaging technique, CrCEST MRI, in individuals with FRDA.  $\tau\text{Cr}$ , an index of skeletal muscle OXPHOS capacity, was prolonged in the LG of adults with FRDA as compared to healthy volunteers, consistent with prior observations that FRDA is associated with decreased skeletal muscle OXPHOS capacity. The association between FRDA and prolonged  $\tau\text{Cr}$  was persistent (Table 7) after accounting potentially relevant clinical covariates, including age and sex, and experimental factors including  $\Delta\text{CrCEST}$ , an index of relative MRI exercise stimulus intensity, and resting CrCEST, an index of free creatine concentration, in statistical models. However, the impact of FRDA on  $\tau\text{Cr}$  was attenuated after accounting for total weekly physical activity, suggesting that inactivity may contribute to decreased skeletal muscle OXPHOS capacity in this condition.

Our findings are consistent with previous reports of decreased skeletal muscle OXPHOS capacity in individuals with FRDA obtained using  $^{31}\text{P}$ -MRS, another MR-based technique that evaluates phosphocreatine metabolism, but whose anatomic resolution is generally more limited than CrCEST MRI [3, 15–17]. Previous  $^{31}\text{P}$ -MRS reports did not include muscle-group-specific estimates. Notably, we found a statistical interaction between muscle group and the effect of disease status on  $\tau\text{Cr}$ , indicating that the effect of disease status on OXPHOS capacity differs by muscle group. This finding highlights the utility of the muscle group-specific CrCEST technique. One potential explanation for muscle group differences in FRDA is that muscle group fiber composition may change as a result of disease. Muscle fiber type switching occurs in diverse metabolic conditions, including muscular dystrophies, type 2 diabetes, obesity [18–20]. At least one study has found changes in fiber type composition in both skeletal and cardiac muscle in a mouse model of FRDA; thus fiber type differences could help explain the muscle group differences we see [21].

Several of our observations also suggest that despite our efforts to personalize and adapt the exercise stimulus, individuals with FRDA performed the exercise testing differently than did healthy controls. First, we found a statistical interaction between disease status and muscle group on  $\Delta\text{CrCEST}$  with exercise, indicating that exercise-related muscle group engagement differs in individuals with FRDA as compared to healthy controls. This difference in muscle engagement is also shown in Supplementary



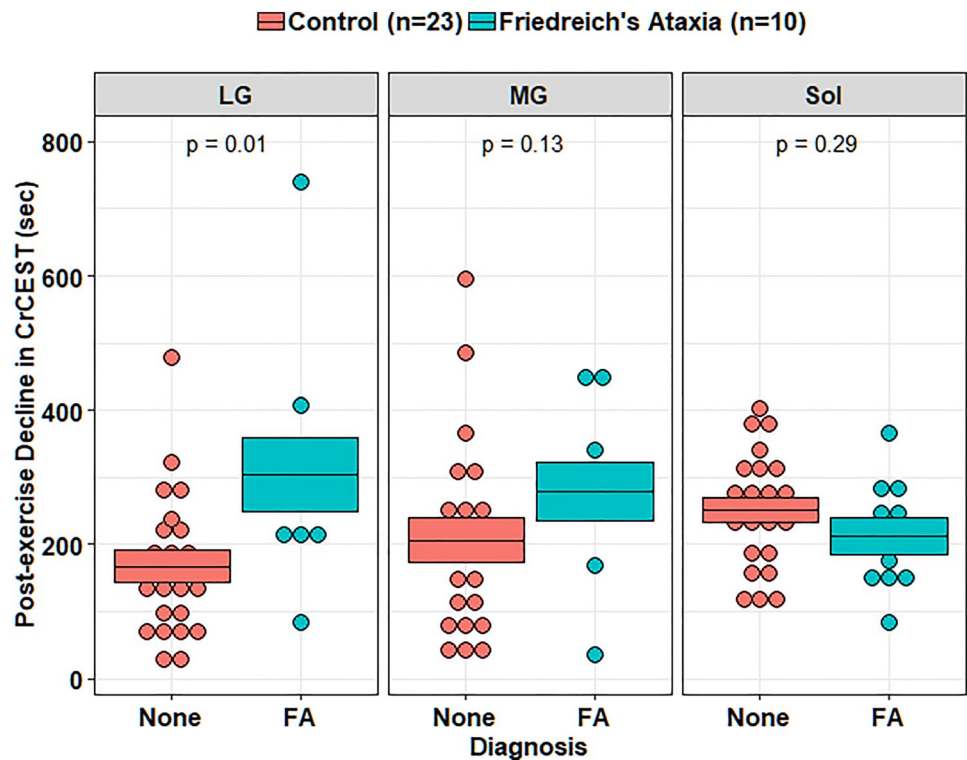
**Fig. 2** Mean CrCEST timeseries for all adults in the (A) lateral gastrocnemius, (B) medial gastrocnemius, and (C) soleus. In the LG, median  $\tau_{Cr}$ =274 s (IQI 221–309 s) in FRDA and  $\tau_{Cr}$ =138 s (IQI 85–226 s) in controls ( $p=0.01$  for difference by Kruskal–Wallis test, Table 2)

Fig. 2. Additionally, when we visually inspected the CrCEST maps, we observed that individuals with FRDA tended to engage all three muscle groups similarly, while healthy controls tended to use the gastrocnemius the most (e.g., Fig. 1). In the context of a plantar flexion exercise,

individuals with FRDA with limited coordination and/or strength may engage all muscle groups, while healthy individuals can efficiently perform the exercise using predominantly the most appropriately positioned muscle group(s). Of note, while we did not include anterior lower



**Fig. 3** Post-exercise  $\tau$ Cr in adults. Orange corresponds to controls, and blue corresponds to adults with FRDA. Median  $\tau$ Cr in the LG was 138 s (IQI = 85–227 s) in controls and 274 s (IQI = 221–309 s) in FRDA (Table 2). In a linear regression analysis, FRDA disease status prolongs  $\tau$ Cr by 131 s (95% CI = 28–234 s) in the LG, accounting for sex and age ( $p = 0.01$ , Table 3). This boxplot also illustrates the interaction between disease status and muscle group described, namely that disease-specific differences in post-exercise  $\tau$ Cr in adults with FRDA are distinct in soleus as compared to LG. LG: lateral gastrocnemius, MG: medial gastrocnemius, Sol: soleus



**Table 5** Adults with FRDA vs. healthy controls, linear regression models of post-exercise decline in CrCEST ( $\tau$ Cr, in seconds) in the lateral gastrocnemius, where prolonged  $\tau$ Cr suggests decreased OXPHOS capacity

Covariate	Model 1 $\beta$ [CI]	Model 2 $\beta$ [CI]	Model 3 $\beta$ [CI]
Age (years)	2 [-2, 6]	-1 [-5, 3]	3.9 [0, 8]
Male sex (vs. female)	86 [-21, 194]	91 [-25, 208]	<b>107</b> <b>[0, 215]*</b>
FRDA (vs. no FRDA)	<b>131*</b> <b>[28, 234]</b>	<b>131*</b> <b>[8, 253]</b>	76 [-45, 196]
$\Delta$ CrCEST w/ Exercise	-	0 [-15, 15]	-
Resting CrCEST	-	-1 [-43, 41]	-
Total Physical Activity (MET-hrs/wk)	-	-	-5 [-10, 1]

For all models,  $n = 32$  participants contributed a total of  $n = 32$  observations. The following covariates were included: Model 1, age, sex, and disease status (no additional covariates); Model 2, age, sex, disease status,  $\Delta$ CrCEST, and resting CrCEST; Model 3, age, sex, disease status, and total physical activity.  $\beta$  values are shown, with corresponding 95% confidence intervals. Results in bold text indicate statistically significant  $\beta$  coefficient values: \* $p < 0.05$ ; \*\* $p < 0.01$ ; \*\*\* $p < 0.001$

leg muscles (e.g., tibialis anterior) in this analysis since they are associated with the dorsiflexion movement, some participants with FRDA can be seen exercising anterior leg muscles, including the individual in Fig. 1B. Engagement of the anterior muscles may be another marker of poor muscle coordination, which occurs in FRDA and likely adversely impacts muscle synergy when performing the plantar flexion movement [1, 22]. Individuals with FRDA may also be weaker, either due to underlying disease and/or deconditioning; indeed, we demonstrated that more self-reported habitual exercise is associated with larger  $\Delta$ CrCEST with plantar flexion.

Waist circumference and self-reported physical activity were also associated with muscle group-specific exercise parameters, independent of FRDA disease status (Table 4, Supplementary Table 1). Across all participants, more time spent in physical activity was associated with shorter  $\tau$ Cr in the MG, suggesting that physical activity is associated with increased OXPHOS capacity in this muscle group. Also, more time spent in physical activity was associated with larger  $\Delta$ CrCEST with exercise in the LG, indicating that  $\Delta$ CrCEST may be an index of exercise performance corresponding to increased capacity to depress a pedal in response to individualized resistance. Overall, healthy volunteers also reported more total physical activity (as well as more time

spent light- and heavy-intensity exercise) than individuals with FRDA. Exercise intolerance is a common symptom in FRDA and in genetic primary mitochondrial disorders [23–25], and exercise therapy is commonly recommended for patients with mitochondrial disease [26]. Future studies including more detailed assessments of exercise capacity and usual physical activity could add to our understanding. Although there is anecdotal evidence that exercise may be therapeutic in FRDA, the potential benefits of exercise in FRDA for muscle remain the focus of investigation [27]. Another index of adverse cardiometabolic health, larger waist circumference, was associated with smaller  $\Delta\text{CrCEST}$  in the MG and soleus in the entire cohort [28, 29]. Overall, these results demonstrate that physical activity and body composition have meaningful associations with muscle metabolic parameters and may explain some disease-specific effects.

Across all participants, resting CrCEST was higher in soleus as compared to LG, even after accounting for a variety of potentially relevant covariates [30]. Higher resting CrCEST in the soleus (relative to the LG) is consistent with our group's previous study assessing OXPHOS in healthy individuals and individuals with diverse mitochondrial diseases [9]. Our findings suggest that the soleus has a higher concentration of free creatine relative to the LG, which may be because the soleus muscle is generally observed to have a higher density of slow twitch, oxidative myofibers [31, 32]. Fast twitch fibers have greater PCr content at rest, so our finding may reflect differences in total creatine and/or creatine metabolism between muscle groups with different fiber types [31]. These findings also demonstrate the utility of measuring free creatine, which is not typically measured in muscle energetics studies, and may provide insight into other processes, such as alterations in creatine transport, that could underlie disease-related metabolic deficits. Also, independent of disease status, resting CrCEST was negatively associated with BMI, even after accounting statistically for sex and age (Table 3). We speculate that excess adiposity in overweight/obese individuals may lead to excess accumulation of intramuscular fat and effective displacement of Cr. We tested a separate statistical model including both right leg fat mass and lean mass in an attempt to dissociate the effects of high fat mass versus high lean mass, since individuals with high BMI tend to have higher amounts of both tissue types, but our model lacked sufficient statistical power to discern independent effects.

This study had several limitations. First, even the careful steps we took to individualize the exercise stimulus did not prevent cohort specific differences in the muscle group pattern of  $\Delta\text{CrCEST}$  with exercise. Since our priority measure in this study is  $\tau\text{Cr}$ , it would have been optimal to use an

exercise stimulus that produced a more similar  $\Delta\text{CrCEST}$  pattern in FRDA versus controls. However, we speculate that inherent disease-specific differences in muscle coordination led to different patterns of muscle engagement that are difficult to eliminate. As previously mentioned, we also did not include anterior lower leg muscles in our analysis, which may provide further insight into muscle coordination in FRDA. With respect to the exercise, the ergometer is calibrated for participants to perform a mild exercise, in part because exercise-induced changes in pH may have effects on CEST signal that are not yet well understood. Thus, another limitation of this study is that we did not measure changes in pH exercise to ensure that in individuals with FRDA, mild exercise does not significantly change pH. Although in our previous study of adults with mitochondrial diseases, pH changes were measured and found to be small with this exercise paradigm [9]. Ultimately, within-participant comparisons of  $\tau\text{Cr}$  over time with consistent provocative exercise stimuli may be more relevant than differences between individuals with FRDA and controls, between whom the exercise stimulus may be challenging to standardize [33]. Nevertheless, work in this area is ongoing in adults as well as in children, in whom further adaptations to the exercise stimulus are needed. Another technical limitation is the reproducibility of manual segmentation of the muscle groups. Our group previously assessed the inter-observer reproducibility of muscle segmentation in CrCEST, and the mean coefficient of variation for tracing the LG was 14.7% [34]. Lastly, our sample size in this rare disorder limited us from constructing larger statistical models to examine the potential independent contributions of multiple other relevant clinical covariates.

In conclusion, this study had several key findings. We found that individuals with FRDA had a prolonged  $\tau\text{Cr}$  compared to controls in the LG, suggestive of decreased OXPHOS capacity, even after accounting statistically for technical factors, including differences in how exercise was performed. However, after accounting for differences in physical activity between cohorts, differences in  $\tau\text{Cr}$  were attenuated, highlighting challenges of detecting the differences between primary (i.e., genetic) and secondary (i.e., related to decreased mobility) adverse effects on muscle metabolism. Optimization of technical factors, including further individualization of the exercise stimulus, may improve the feasibility and utility of CrCEST imaging for noninvasive assessment of OXPHOS capacity. Ultimately, within-individual comparisons over time in  $\tau\text{Cr}$  may be most informative. We envision continued development of this metabolic imaging tool.

**Supplementary Information** The online version contains supplementary material available at <https://doi.org/10.1007/s00415-021-10821-1>.

**Acknowledgements** The project described was supported by the National Center for Research Resources and the National Center for Advancing Translational Sciences, National Institutes of Health, through grants 5UL1TR001878-05, 5K23DK102659-03, 5R03DK114491-02, and 1T32GM136573-01, and the Friedreich's Ataxia Research Alliance. The content is solely the responsibility of the authors and does not necessarily represent the official views of the National Institutes of Health. Procedures were conducted in the CHOP/HUP Center for Human Phenomic Science (CHPS). We thank participants and families for their participation and support.

## Declarations

**Conflicts of interest** Ravinder Reddy is a co-inventor on patent "CEST MRI Methods for Imaging of Metabolites and the Use of Same as Biomarkers." Neil Wilson is currently an employee of Siemens Medical Solutions USA. All other authors have no conflict of interest to declare.

**Ethical standard** This study was performed under an approved Institutional Review Board protocol of the University of Pennsylvania (clinicaltrials.gov: NCT02154711) and was conducted according to the Declaration of Helsinki. Written, informed consent for all participants were obtained.

**Open Access** This article is licensed under a Creative Commons Attribution 4.0 International License, which permits use, sharing, adaptation, distribution and reproduction in any medium or format, as long as you give appropriate credit to the original author(s) and the source, provide a link to the Creative Commons licence, and indicate if changes were made. The images or other third party material in this article are included in the article's Creative Commons licence, unless indicated otherwise in a credit line to the material. If material is not included in the article's Creative Commons licence and your intended use is not permitted by statutory regulation or exceeds the permitted use, you will need to obtain permission directly from the copyright holder. To view a copy of this licence, visit <http://creativecommons.org/licenses/by/4.0/>.

## References

- Pandolfo M (2008) Friedreich ataxia. *Arch Neurol* 65(10):1296–1303
- Martelli A, Puccio H (2014) Dysregulation of cellular iron metabolism in Friedreich ataxia: from primary iron-sulfur cluster deficit to mitochondrial iron accumulation. *Front Pharmacol* 5:130
- Lodi R, Cooper JM, Bradley JL et al (1999) Deficit of in vivo mitochondrial ATP production in patients with Friedreich ataxia. *Proc Natl Acad Sci USA* 96(20):11492–11495
- Lanza IR, Bhagra S, Nair KS, Port JD (2011) Measurement of human skeletal muscle oxidative capacity by 31P-MR spectroscopy: a cross-validation with in vitro measurements. *J Magn Reson* 34(5):1143–1150
- Zierath JR, Hawley JA (2004) Skeletal muscle fiber type: influence on contractile and metabolic properties. *PLoS Biol* 2(10):e348
- Kogan F, Hariharan H, Reddy R (2013) Chemical exchange saturation transfer (CEST) imaging: description of technique and potential clinical applications. *Curr Radiol Rep* 1(2):102–114
- Van Zijl PC, Yadav NN (2011) Chemical exchange saturation transfer (CEST): what is in a name and what isn't? *Magn Reson Med* 65(4):927–948
- Kogan F, Haris M, Singh A et al (2014) Method for high-resolution imaging of creatine in vivo using chemical exchange saturation transfer. *Magn Reson Med* 71(1):164–172
- DeBrosse C, Nanga RP, Wilson N et al (2016) Muscle oxidative phosphorylation quantitation using creatine chemical exchange saturation transfer (CrCEST) MRI in mitochondrial disorders. *JCI Insight*. 1(18):e88207
- Feldman HI, Appel LJ, Chertow GM et al (2003) The Chronic renal insufficiency cohort (CRIC) study: design and methods. *J Am Soc Nephrol JASN*. 14(7Suppl 2):S148–S153
- Kim M, Gillen J, Landman BA et al (2009) Water saturation shift referencing (WASSR) for chemical exchange saturation transfer (CEST) experiments. *Magn Reson Med* 61:1441–1450
- Volz S, Nöth U, Rotarska-Jagiela A, Deichmann R (2010) A fast B1-mapping method for the correction and normalization of magnetization transfer ratio maps at 3 T. *Neuroimage* 49(4):3015–3026
- Wilson NE (2016) ExerciseCEST. Zenodo. <https://doi.org/10.5281/zenodo.59640>. Aug 4
- North American Association for the Study of Obesity, National Heart, Lung, Blood Institute, & NHLBI Obesity Education Initiative (2000) The practical guide: identification, evaluation, and treatment of overweight and obesity in adults. National Institutes of Health, National Heart, Lung, and Blood Institute, NHLBI Obesity Education Initiative, North American Association for the Study of Obesity.
- Vorgerd M, Schöls L, Hardt C et al (2000) Mitochondrial impairment of human muscle in Friedreich ataxia in vivo. *Neuromuscul Disord* 10(6):430–435
- Schöls L, Vorgerd M, Schillings M et al (2001) Idebenone in patients with Friedreich ataxia. *Neurosci Lett* 306(3):169–172
- Nachbauer W, Boesch S, Schneider R et al (2013) Bioenergetics of the calf muscle in Friedreich ataxia patients measured by 31P-MRS before and after treatment with recombinant human erythropoietin. *PLoS ONE* 8(7):e69229
- Ciciliot S, Rossi AC, Dyar KA et al (2013) Muscle type and fiber type specificity in muscle wasting. *Int J Biochem Cell Biol* 45(10):2191–2199
- Oberbach A, Bossenz Y, Lehmann S et al (2006) Altered fiber distribution and fiber-specific glycolytic and oxidative enzyme activity in skeletal muscle of patients with type 2 diabetes. *Diabetes Care* 29(4):895–900
- Coppola G, Marmolino D, Lu D et al (2009) Functional genomic analysis of frataxin deficiency reveals tissue-specific alterations and identifies the PPAR $\gamma$  pathway as a therapeutic target in Friedreich's ataxia. *Hum Mol Genet* 18(13):2452–2461
- Tanner CJ, Barakat HA, Dohm GL et al (2002) Muscle fiber type is associated with obesity and weight loss. *Am J Physiol Endocrinol Metabol* 282(6):E1191–E1196
- Wakeling JM, Blake OM, Wong I et al (2011) Movement mechanics as a determinate of muscle structure, recruitment and coordination. *Philosoph Trans Royal Soc B Biol Sci* 366(1570):1554–1564
- Jeppesen TD, Schwartz M, Olsen DB et al (2006) Aerobic training is safe and improves exercise capacity in patients with mitochondrial myopathy. *Brain* 129(12):3402–3412
- Tarnopolsky MA, Raha S (2005) Mitochondrial myopathies: diagnosis, exercise intolerance, and treatment options. *Med Sci Sports Exerc* 37(12):2086–2093
- Drinkard BE, Keyser RE, Paul SM et al (2010) Exercise capacity and idebenone intervention in children and adolescents with Friedreich ataxia. *Arch Phys Med Rehabil* 91(7):1044–1050
- Parikh S, Goldstein A, Koenig MK et al (2015) Diagnosis and management of mitochondrial disease: a consensus statement from the Mitochondrial Medicine Society. *Genet Med* 17(9):689–701

27. Zhao H, Lewellen BM, Wilson RJ et al (2020) Long-term voluntary running prevents the onset of symptomatic Friedreich's ataxia in mice. *Sci Rep* 10(1):1–1
28. Vazquez G, Duval S, Jacobs DR Jr, Silventoinen K (2007) Comparison of body mass index, waist circumference, and waist/hip ratio in predicting incident diabetes: a meta-analysis. *Epidemiol Rev* 29(1):115–128
29. Savva SC, Tornaritis M, Savva ME et al (2000) Waist circumference and waist-to-height ratio are better predictors of cardiovascular disease risk factors in children than body mass index. *Int J Obes* 24(11):1453–1458
30. Johnson M, Polgar J, Weightman D, Appleton D (1973) Data on the distribution of fibre types in thirty-six human muscles: an autopsy study. *J Neurol Sci* 18(1):111–129
31. Gollnick PD, Sjödin B, Karlsson J et al (1974) Human soleus muscle: a comparison of fiber composition and enzyme activities with other leg muscles. *Pflügers Arch* 348(3):247–255
32. Tesch PA, Thorsson A, Fujitsuka N (1989) Creatine phosphate in fiber types of skeletal muscle before and after exhaustive exercise. *J Appl Physiol* 66(4):1756–1759
33. Papa S (1996) Mitochondrial oxidative phosphorylation changes in the life span. Molecular aspects and physiopathological implications. *Biochimica et Biophysica Acta (BBA)-Bioenergetics*. 1276(2):87–105
34. Zamani P, Proto EA, Wilson N et al (2021) Multimodality assessment of heart failure with preserved ejection fraction skeletal muscle reveals differences in the machinery of energy fuel metabolism. *ESC Heart Fail*. <https://doi.org/10.1002/ehf2.13329>